# HIGHLY-EXCITED NORMAL AND SUPER-DEFORMED ROTATING NUCLEI STUDIED WITH E1 AND E2 $\gamma$-CONTINUUM MEASUREMENTS* **

A. Bracco[a,b], F. Camera[a,b], S. Frattini[a,b], S. Leoni[a,b], B. Million[a,b], A. Maj[c], M. Kmiecik[c], B. Herskind[d] and M. Bergström[d]

[a] Dipartimento di Fisica, Università di Milano
Via Celoria 16, 20133 Milan, Italy
[b] Istituto Nazionale di Fisica Nucleare, sezione di Milano, Italy
[c] The Henryk Niewodniczański Institute of Nuclear Physics
Radzikowskiego 152, 31-342 Kraków, Poland
[d]The Niels Bohr Institute
Blegdamsvej 17, Copenhagen DK-2100 Ø, Denmark

*(Received February 2, 1999)*

The $\gamma$-decay in the continuum region and of both E1 and E2 types is investigated to learn about the properties of hot and warm rotating nuclei. In particular, two topics concerning highly excited nuclei are discussed. The first is the search for the $\gamma$-decay of the Giant Dipole Resonance built on superdeformed (SD) nuclear configurations of $^{143}$Eu. The available results seem to indicate that the superdeformation survives only few MeV above the yrast line. The second topic concerns the measurement the rotational quadrupole moment of thermally excited high spin states in $^{168}$Yb. A new technique, based on fluctuation analysis has been employed which has provided for the first time the value of the quadrupole moment from continuous spectra.

PACS numbers: 21.10.Re, 21.60.Ka, 23.20.Lv, 27.60.+q

## 1. Introduction

Information on the properties of warm and hot rotating nuclei can be obtained through the study of the unresolved continuum spectra. In particular, the analysis of quasi-continuum of E2 character, forming ridge and valley structures in $\gamma$-coincident spectra (in the region $0.7<E_\gamma<1.5$ MeV)

* Presented at the XXXIII Zakopane School of Physics, Zakopane, Poland, September 1–9, 1998.

** Partial financial support from the Polish State Committee for Scientific Research (KBN Grant No. 2 P03B 001 16.)

has provided information on effects beyond-mean field such as that of the rotational band mixing induced by residual interaction. Conversely, the study of high energy $\gamma$-rays in the region $5 < E_\gamma < 20$ MeV emitted by the giant dipole resonance (GDR) provides information on the the shape of hot nuclei and on the damping mechanisms of this collective mode.

In the following sections two different topics, one concerning the GDR built on excited states and the other concerning the rotational band mixing problem are discussed. The first is the search for the $\gamma$-decay of the Giant Dipole Resonance built on superdeformed (SD) nuclear configurations of $^{143}$Eu. The second concerns the measurement of the rotational quadrupole moment of thermally excited high spin states in $^{168}$Yb.

## 2. The GDR in superdeformed nuclei

One of the important problems not yet understood concerning superdeformed nuclei is how these nuclear configurations are populated. It has been suggested [1] that the rather intense population of superdeformed bands (of the order of 1%) is connected to the E1 cooling of the nucleus that is expected to be enhanced due to the large splitting of the GDR strength function and to the level density of the superdeformed states.

The first study aiming at searching for a signal of the $\gamma$-decay of the GDR in the superdeformed nucleus was done for the $^{143}$Eu case. This nucleus is characterized by a very intense continuum of E2 type that was found to originate from superdeformed configurations and to have a decay path feeding only particular low-spin states [2]. At low spins, due to the coexistence of both spherical (ND) and triaxially deformed (TD) shapes [3,4], this nucleus has a very complex and irregular level scheme and it becomes superdeformed (SD) at high spins.

Both the SD yrast band and the excited SD states forming the E2 continuum follow decay routes leading to the ground state, that populate low spin states of the spherical shape only (ND). It is therefore expected that one should see the $\gamma$-decay of the GDR built on superdeformed states by comparing the high-energy $\gamma$-spectrum gated by low spin ND transitions (populated by the SD decay) with that gated by low spin TD transitions (not populated by the SD decay). A schematic picture of the decay is given in figure 1.

The results of the experiment, described in [5] and performed using the $^{37}$Cl + $^{110}$Pd at 165 MeV are displayed in figure 2.

The two high-energy $\gamma$-spectra, one gated by ND transitions and the other by TD transitions and associated to the fold interval 6-10 measured with the multiplicity filter ($\langle I \rangle \approx 45\ \hbar$), are compared in Fig. 2. They are different in the region $7 < E_\gamma < 10$ MeV.

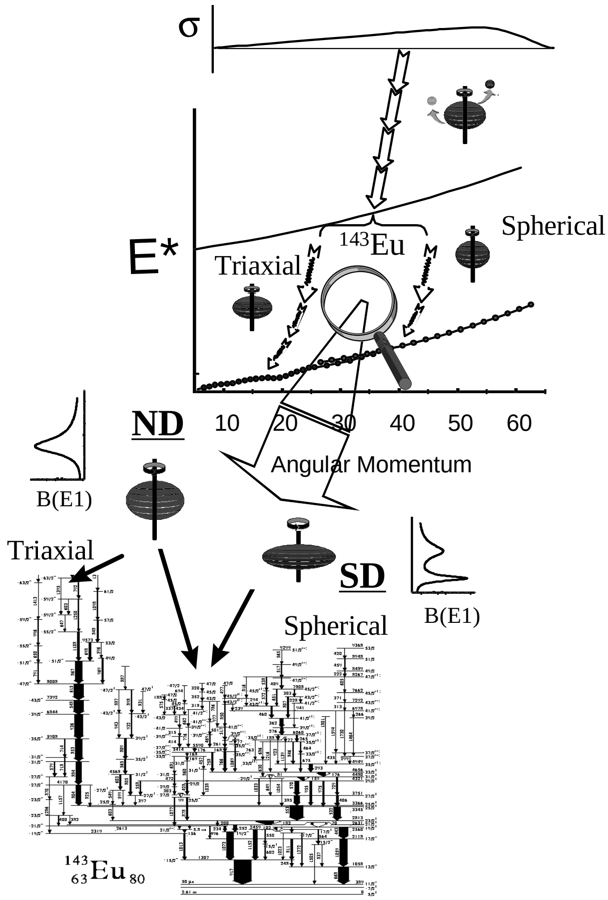


Fig. 1. Schematic illustration of $\gamma$-decay of the GDR in excited nuclei leading to the population of specific final states of the same residual nucleus characterized by different deformations.

The ratio of the ND gated with TD gated spectra , displayed in the inset of figure 2, shows some excess (of the order of 15 to 35 %) in the region where one expects to find the low energy component (dipole vibration along the symmetry axis) of the GDR built on a superdeformed configuration.

Statistical model predictions of the ratio spectrum were also obtained. We denote with $Y_{\rm ND}(E_\gamma)$ the calculation correponding to the normally deformed nucleus and with $Y_{\rm SD}(E_\gamma)$ the calculation corresponding to the superdeformed configuration.

The $Y_{\rm ND}(E_\gamma)$ yield was obtained assuming that the GDR strength function is a a single Lorentzian with centroid $E_{\rm GDR}$= 15 MeV and width $\Gamma_{\rm GDR}$ varying, with increasing excitation energy, from 5 to 8 MeV. The $Y_{\rm SD}(E_\gamma)$

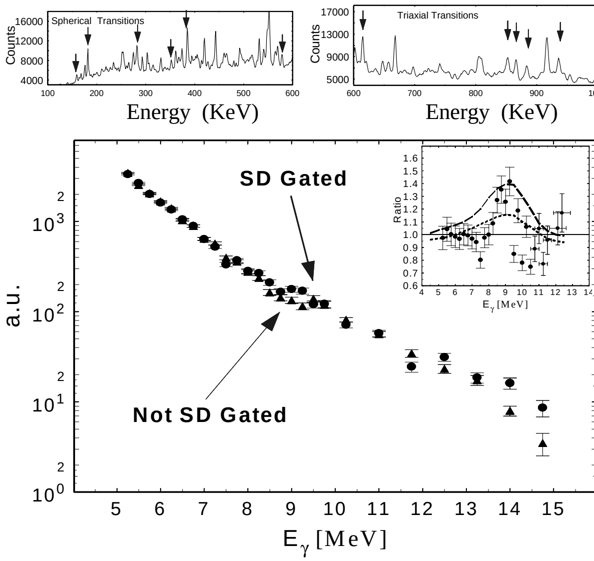


Fig. 2. High energy spectra measured with the $BaF_2$ detectors. One in coincidence with ND transitions (shown in the top part) fed by SD decay (filled circles) and the other is in coincidence with TD transitions (also shown in the top part) not fed by SD decay (filled triangles). In the inset the ratio between the two spectra is shown together with the statistical model calculations described in the text.

yield was obtained in the same way as the $Y_{\mathrm{ND}}(E_\gamma)$ yield, with the exception that in the angular momentum region $40\hbar < I < 55\hbar$ and for energy $U$ above yrast in the interval $U = 0$-$15$ MeV, the GDR strength function was assumed to be a superposition of two Lorentzian functions. In particular, for the dipole vibration along the symmetry axis we have used $E_{\mathrm{GDR(low)}} = 9.5$ MeV and $\Gamma_{\mathrm{GDR(low)}} = 2.5$ MeV , and 33% of the energy weighted sum rule strength (EWSR) and for the dipole vibrations perpendicular to the symmetry axis $E_{\mathrm{GDR(Hi)}} = 18.5$ MeV and $\Gamma_{\mathrm{GDR(Hi)}} = 6.5$ MeV, and 66% of the EWSR.

Using the calculated $Y_{\mathrm{ND}}(E_\gamma)$ and $Y_{\mathrm{SD}}(E_\gamma)$ yields and assuming that 40% of the total decay flux passes through the superdeformed states, we have computed the ratio:

$$Y_{\mathrm{ratio}}(E_\gamma) = \frac{0.4 \times Y_{\mathrm{SD}}(E_\gamma) + 0.6 Y_{\mathrm{ND}}(E_\gamma)}{Y_{\mathrm{ND}}(E_\gamma)} . \tag{1}$$

Since the $E1$ decay depends on the density of states, the ratio spectrum was calculated for two different sets of values for the levels density parameters $a_{\mathrm{SD}}$ and $a_{\mathrm{ND}}$ [1]. In Fig. 2a, the calculation corresponding to $a_{\mathrm{SD}} = a_{\mathrm{ND}}$

= A/8 MeV$^{-1}$ (dash-line) is shown in comparison with the data and with a calculation with $a_{\mathrm{SD}}$ = A/10 MeV$^{-1}$ and $a_{\mathrm{ND}}$ = A/8 MeV$^{-1}$ (full drawn line). The magnitude of the measured yield lies between the two predictions.

It is important to stress that the transition probability for the E1 decay for the SD nucleus is a factor of 4 to 10 larger (depending on the assumed value for the superdeformed level density) than that of the ND nucleus and yet, the enhancement in the total ratio spectrum, that receives contributions from all the decay steps of the compound nucleus, is much smaller (only of the order of 15 to 35 %).

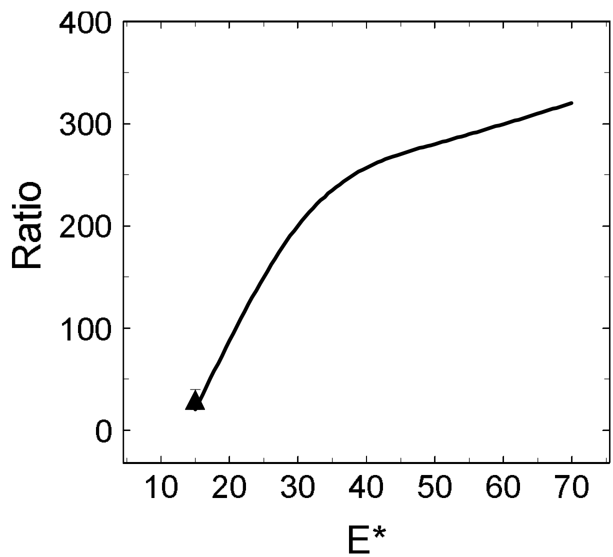


Fig. 3. The ratio of the spectrum including superdeformed GDR in the spin window 40-55 $\hbar$ with the spectrum corresponding to spherical shape as a function of excitation energy.

It is interesting to know the value of the calculated ratio when the interval of excitation energy above the yrast in which the superdeformation is assumed to exist becomes larger. This can be seen in figure 3 where the calculated ratio is shown as a function of excitation energy together with the experimental point (triangle). The experimental value indicates that the nucleus is superdeformed only near to the yrast line. In contrast, if it was superdeformed at the beginning of the compound nucleus the ratio would be more than 10 times larger.

More firm conclusions on this interesting problem are expected to be obtained with the new experiment recently performed with the EUROBALL array.

## 3. The quadrupole moment of the $^{168}$Yb

Several studies of the rotational quasi-continuum for normally deformed nuclei in the rare earth region have been made in the last few years analysing the "ridge-valley" structure in $E_{\gamma_1} \times E_{\gamma_2}$ spectra [6]. These studies have shown that the rotational motion is carried by regular rotational bands at low excitation energy, followed by a transition to strongly mixed bands at the densely spaced levels at higher excitation energy. By comparing the experimental data with predictions of the rotational damping model [7], one has learned that the mixing among rotational bands is strongly governed by a residual interaction including high multipole terms, and that the mixing is configuration dependent [8-9].

In spite of the progress made recently in this field, one of the basic assumptions behind the rotational damping model, namely that the warm nucleus is strongly collective with a quadrupole moment $Q_t$ of the same order of that of the cold regular rotational bands, has never been experimentally verified. To test this assumption, lifetime measurements of the damped transitions are necessary.

So far, lifetimes of discrete high spin states have been measured by employing the Doppler Shift Attenuation Method (DSAM). In addition, the fractional Doppler shifts of the regular bands forming ridge structures in $E_{\gamma_1} \times E_{\gamma_2}$ spectra, and of the unresolved high energy rotational transitions forming the upper edge of the E2 bump in one dimensional (1D) spectra, have been measured [10]. However, only for the ridges and for the discrete lines it has been possible to deduce the value of $Q_t$, since the high energy transitions at the edge of the E2 bump were found to be fully shifted and consequently no sensitivity to the value of the quadrupole moment was obtained.

To deduce the quadrupole moment in the region of strongly mixed bands a method, based on the *fluctuation pattern* of counts of unresolved transitions in the diagonal valley of $E_{\gamma_1} \times E_{\gamma_2}$ spectra, was developed and employed [11]. By focusing on the valley, we select damped transitions in the most clean way, excluding transitions which display the energy correlations characteristic of regular rotational bands. A Doppler shift analysis of the fluctuation patterns is made through a covariance analysis of shifted counts in the valley.

The fusion reaction $^{30}$Si + $^{138}$Ba $\Rightarrow$ $^{168}$Yb was used to populate the residues $^{163,164,165}$Yb after xn evaporations. The experiment was carried out at the Institut de Recherches Subatomiques of Strasbourg using the Vivitron tandem accelerator and the multidetector system EUROGAM II. Two runs were made, one with a backed $^{138}$Ba target of 225 $\mu$g/cm$^2$ evaporated on a Pb-backing of 9 mg/cm$^2$, the other using a stack of two targets each evaporated on a thin Au foil of $\approx 580$ $\mu$g/cm$^2$. The total thickness of the $^{138}$Ba was 450 $\mu$g/cm$^2$. The initial velocity of the residual nuclei in the middle of the target was calculated to be $v/c = 1.8\%$. The residual nucleus $^{164}$Yb was most strongly populated (approximately 70% at high spin), reaching a maximum angular momentum calculated to be $63\hbar$. A total of 220 and 120 M triple and higher-fold events (with an average Ge-fold of 5) were collected in the thin and backed target experiments, respectively. Energy-dependent time gates on the Ge time signal were used to suppress background from neutrons.

The data were sorted into 2D spectra, namely $(E^{\rm F}_{\gamma_1} \times E^{\rm B}_{\gamma_2})$ and $(E^{\rm B}_{\gamma_1} \times E^{\rm F}_{\gamma_2})$, where B and F indicate backward and forward angles, respectively. Two sets of spectra were then constructed. The first consists of spectra of the type $(E^{\rm B}_{\gamma_1} \times E^{\rm F}_{\gamma_2})_{\rm Shift=\mathit{N}}$, obtained by shifting the counts in channel $(X,Y)$ to channel $(X+N,\ Y-N)$, each corresponding to given integer values, $N = 1,2,3\ldots$. The second set consists of spectra of the type $(E^{\rm F}_{\gamma_1} \times E^{\rm B}_{\gamma_2})_{\rm Shift=-\mathit{N}}$, obtained by shifting the counts in channel $(X,Y)$ to channel $(X-N, Y+N)$.

The correlations in fluctuations between any two $(E^{\rm B}_{\gamma_1} \times E^{\rm F}_{\gamma_2})_{\rm Shift=\mathit{N}}$ and $(E^{\rm F}_{\gamma_1} \times E^{\rm B}_{\gamma_2})_{\rm Shift=-\mathit{N}}$ spectra (denoted in the following equation by $M(A)$ and $M(B)$) were evaluated in terms of the covariance of counts, defined as:

$$\mu_{2,\rm cov}(A,B) \equiv \frac{1}{N_{\rm ch}} \sum_j (M_j(A) - \tilde{M}_j(A))(M_j(B) - \tilde{M}_j(B))\,. \qquad (2)$$

The sum is over a region spanning $N_{\rm ch}$ channels in a $2D$ 60 keV $\times$ 60 keV window, and $\tilde{M}$ denotes an average spectrum (which in our case is found by the routine STATFIT as a numerical smoothed third-order approximation to the $2D$ spectrum [6,12]).

To normalize the covariance and thereby determine the degree of correlation between the two spectra, the correlation coefficient $r(A,B)$ was calculated:

$$r(A,B) \equiv \frac{\mu_{2,\rm cov}(A,B)}{\sqrt{(\mu_2(A) - \mu_1^{\rm (raw)}(A))(\mu_2(B) - \mu_1^{\rm (raw)}(B))}}\,. \qquad (3)$$

Here, $\mu_1^{\rm (raw)}$ is the first moment of the raw spectrum, and $\mu_2$ is the second moment of the COR-subtracted spectrum, both defined for the same region $N_{\rm ch}$, as the covariance. The second moment is related to the covariance by the relation $\mu_2(A) = \mu_{2,\rm cov}(A,A)$.

The ratio of the value corresponding to the maximum of the correlation coefficient $r$ and to the full shift position, the fractional Doppler shift $F(\tau)$ is deduced. We find an energy region in the valley $800 < E_\gamma < 1000$ keV

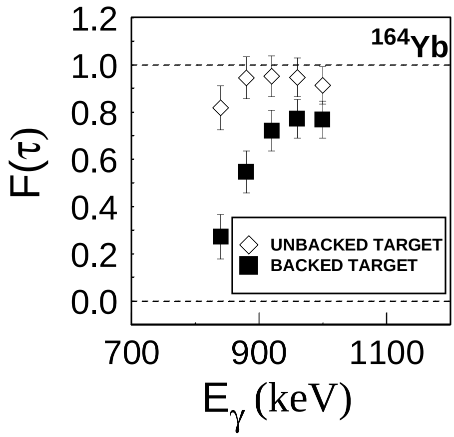


Fig. 4. The fractional Doppler shift obtained for the backed and unbacked target experiments applying the fluctuation analysis technique.

where $F(\tau)$ is significantly smaller than 1 and thereby a sensitivity to the value of the quadrupole moment. As can be seen from Fig. 4, $F(\tau)$ increases with $\langle E_\gamma \rangle$, as expected.

A stringent test of this new method is obtained by analyzing data for the same reaction but using a thin target. In fact, in the case of thin target data one expects to find $F(\tau) \approx 1$ for all $\gamma$-transition energies because the emission from the recoiling nucleus occurs in flight with the maximum velocity. The results of the analysis of the backed and thin target data are shown in Fig. 4. In the figure we compare data corresponding to the same average transition energy for a backed and a thin target. Indeed, while the backed target data display partial shifts, the thin target data are in accordance with the full shifts, giving a convincing support to the validity of the new method.

The observed Doppler shift attenuation corresponds to effective decay times related to the history of the paths from the entry point to the time of emission of the observed transitions. The $\gamma$ cascades proceed through the region of rotational damping, where the energy spread of the decay transitions affects the average lifetimes due to the $E_\gamma^5$ factor in the E2 transition probability. In order to extract the nuclear quadrupole moment $Q_t$ from the measured shifts, the $\gamma$-cascades from the excited nucleus have been realistically simulated by theoretically calculated cascades including damping, starting from an entry distribution in energy and spin of the residual nucleus [13] and ending at the transition energy in question. The competition between statistical E1 transitions, governed by the tail of the GDR resonance, and E2 transitions from microscopically calculated rotational bands is simulated. The energies and transition probabilities of the rotational bands mixed by the residual interaction are available for the $^{168}$Yb nucleus in great detail and have therefore been used to represent typical decay paths in a deformed nucleus in the same mass region [13].

The intrinsic lifetime $\tau_i$ of a state $i$ at spin $I$ and excitation energy $U_i$ was calculated starting from the transition probabilities for E1 and E2 decay $T(\mathrm{E1}, U_i)$ and $T(\mathrm{E2}, U_i)$. The simulation program calculates the effective lifetime $\tau$ of a transition at spin I as the sum of the lifetimes $\tau_i$ of the preceding transitions with spin $J \geq I$, $\tau(I) = \Sigma_{J \geq I} \tau_i(J)$. Making use of the velocity profile of the recoiling nucleus in the target and backing, the program calculates the velocity of the nucleus at the time $\tau$ and then the associated Doppler shift.

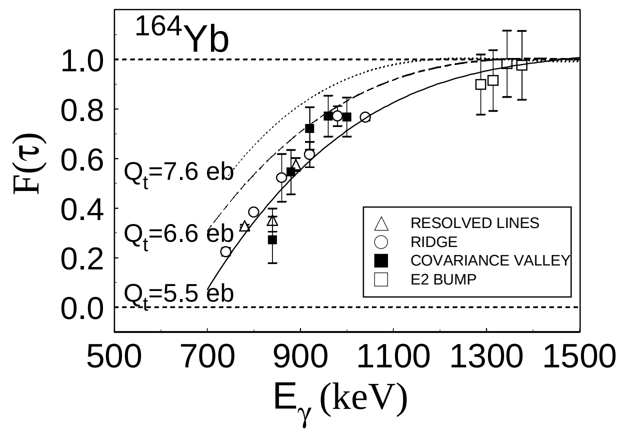


Fig. 5. The Fractional Doppler shift obtained from the analysis of the discrete peaks, ridge and valley structures. The curves are obtained with the simulations described in the text.

In Fig. 5, the experimental data are shown together with the fractional shifts deduced from simulated spectra for three different values of $Q_t = 5.5$, 6.6 and 7.6 eb. One can see that the data are well described by the curve corresponding to $Q_t = 5.5$ b (or 200 W.u.). For this high spin region, similar values of the quadrupole moment were also found in previous works [14,15] using a different reaction and experimental setup, in which Doppler shifts were deduced for both discrete lines and ridge structures.

An important conclusion can be drawn from this work: the discrete excited bands carry the same rotational collectivity as the yrast band, and this collectivity is also maintained for the thermally excited mixed bands up to around 2 MeV of excitation energy above yrast.

For the mixed bands, the lifetime is not only sensitive to the total $Q_t$, but also to the distribution of the transition energy of the fragmented strength. A significant part of the strength might not be available for rotational decay, because it is shifted too far up in excitation energy, and thereby down in transition energy. The present measurement shows that the major part of the strength remains concentrated around the average decay energy.

In summary, a new method based on a covariance analysis of spectra measured with detectors at forward and backward angles has allowed to extract for the first time the quadrupole moment of states in a nucleus with excitation energies in the continuum region. The results show that the nucleus conserves its collectivity at increasing excitation energy ($\leq 2$ MeV), thus giving strong support to the rotational damping model.

## 4. Conclusion

The first measurement aiming at searching the decay of the giant dipole resonance in superdeformed nuclei has given indications that the superdeformation is a property of nuclei near the yrast line. If future experiments confirm this findings it will be important to check in another way the nuclear deformation at few MeV above yrast. This can be done measuring the quadrupole deformation of the E2 continuum.

The technique to be used to perform this type of measurements has been developed and tested in the case of a normal deformed nucleus $^{164}$Yb. The results in that case show that the nucleus conserves its collectivity and deformation at few MeV above yrast, thus giving strong support to the rotational damping model.

REFERENCES

[1] B. Herskind *et al.*, *Phys. Rev. Lett.* **59**, 2416 (1987).
[2] S. Leoni *et al.*, *Phys. Rev. Lett.* **76**, 3281 (1996).
[3] A. Atac *et al.*, *Phys. Rev. Lett.* **70**, 1069 (1993).
[4] M. Piiparinen *et al.*, *Z. Phys.* **A343**, 367 (1992).
[5] F. Camera *et al.*, *Acta Phys. Pol.* **B28**, 207 (1997).
[6] T. Døssing *et al.*, *Phys. Rep.* **268**, 1 (1996).
[7] B. Lauritzen, T. Døssing, R. A. Broglia, *Nucl. Phys.* **A457**, 61 (1986).
[8] M. Matsuo *et al.*, *Nucl. Phys.* **A617**, 1 (1997).
[9] M. Matsuo *et al.*, *Nucl. Phys.* **A620**, 296 (1997).
[10] B. Million *et al.*, *Phys. Lett.* **B415**, 321 (1997).
[11] S. Frattini *et al.*, *Phys. Rev. Lett.* **81**, 2659 (1998).
[12] P. Bosetti *et al.*, *Phys. Rev. Lett.* **76**, 1204 (1996).
[13] A. Bracco *et al.*, *Phys. Rev. Lett.* **76**, 4484 (1996).
[14] I.Y. Lee *et al.*, *Nucl. Phys.* **A554**, 485 (1993).
[15] H. Xie *et al.*, *Nucl. Phys.* **A599**, 560 (1996).